This article has been accepted for publication in a future issue of this journal, but has not been fully edited. Content may change prior to final publication.
Citation information: DOI: 10.1109/JIOT.2025.3610070, IEEE Internet of Things Journal

Recursive Unscented Kalman Filtering for Power Distribution Networks Under Hybrid Attacks: Tackling Dynamic Quantization Effects

Xingzhen Bai, Guhui Li, Zidong Wang, Zhongyi Zhao, and Hongli Dong

***Abstract*—This paper investigates the state estimation problem for power distribution networks subject to dynamic quantization effects and hybrid cyber-attacks, where measurement signals are transmitted from sensors to a remote filter via open digital communication networks. To enhance bandwidth utilization and ensure reliable data transmission, a dynamic quantization mechanism is introduced, which effectively accommodates the dynamic characteristics of power signals. Furthermore, the system is vulnerable to hybrid cyber-attacks that may occur simultaneously in a random manner, including denial-of-service attacks and false data injection attacks, characterized by Bernoulli distributed random variables. The primary objective of this work is to develop a recursive unscented Kalman filter capable of addressing the combined challenges of measurement nonlinearities, dynamic quantization effects, and hybrid cyber-attack scenarios. By solving Riccati-like difference equations, an upper bound on the filtering error covariance is derived, and subsequently minimized through the design of time-varying filter gains. Extensive simulations on the IEEE 69 distribution test system demonstrate the effectiveness of the proposed filtering algorithm.**

***Index Terms*—Power distribution networks, dynamic quantizers, denial-of-service attacks, false data injection attacks, recursive unscented Kalman filtering.**

I. Introduction

Recent years have witnessed significant dynamic evolution in power distribution networks (PDNs), primarily driven by the integration of distributed generation sources, the incorporation of flexible loads, and advancements in communication technologies. These developments have fundamentally altered the operational paradigm of PDNs, necessitating the development of advanced monitoring systems capable of maintaining accurate state estimation under increasingly complex operating conditions. State estimation techniques have emerged as essential components in modern PDN monitoring infrastructure, providing foundational data to support various operational functions, including current calculations, fault diagnosis, and bad data detection [12], [17], [38]. The accuracy and reliability of state estimation directly impact the effectiveness of these functions, thereby influencing overall system performance. Given the growing complexity of PDNs and their increasing reliance on precise operational data, developing robust state estimation methodologies has become essential for ensuring system efficiency and reliability [5], [27].

State estimation methodologies have undergone significant evolution in recent decades, primarily categorized into static and dynamic estimation paradigms. While traditional static methods have demonstrated utility in certain applications, their inherent limitations have become particularly apparent when applied to modern PDNs, due to their complex characteristics including time-varying dynamics, strong nonlinearities, and rapidly changing operating conditions. To address these challenges, dynamic state estimation techniques have been developed as a more robust framework for PDN monitoring [6], [14], [47]. These methods systematically incorporate both real-time measurement data and system dynamics models to provide accurate state tracking and predictive capabilities. Among various dynamic estimation approaches, unscented Kalman filtering (UKF) has emerged as particularly effective for power system applications. The effectiveness stems from the use of the unscented transformation techniques, which provides superior approximation of nonlinear system statistics compared with traditional linearization methods. Consequently, the application of UKF in PDN state estimation represents a natural choice.

In digital communication systems for PDNs, signal quantization represents a critical preprocessing step to optimize bandwidth utilization. Conventional static quantization methods, despite their widespread adoption in engineering applications due to implementation simplicity and computational efficiency [1], [48], demonstrate significant limitations when processing dynamic measurement signals. The primary constraint stems from their fixed quantization thresholds, which

This work was supported in part by the National Natural Science Foundation of China under Grants 61933007, 62273211, 62403130, and U21A2019; in part by the Jiangsu Provincial Scientific Research Center of Applied Mathematics under Grant BK20233002; in part by the Natural Science Foundation of Jiangsu Province of China under Grant Number BK20241286; in part by the Jiangsu Funding Program for Excellent Postdoctoral Talent of China under Grant Number 2024ZB601; in part by the China Postdoctoral Science Foundation-CCTEG Joint Support Program under Grant Number 2025T055ZGMK; in part by the China Postdoctoral Science Foundation-CCTEG Joint Support Program under Grant Number 2025T055ZGMK; in part by the Royal Society of the UK; and in part by the Alexander von Humboldt Foundation of Germany. *(Corresponding author: Zidong Wang)*

Xingzhen Bai and Guhui Li are with the College of Electrical Engineering and Automation, Shandong University of Science and Technology, Qingdao 266590, China. (Emails: xzbai@163.com; lgh_sdust@163.com).

Zidong Wang is with the College of Electrical Engineering and Automation, Shandong University of Science and Technology, Qingdao 266590, China; and is also with the Department of Computer Science, Brunel University London, Uxbridge, Middlesex, UB8 3PH, United Kingdom. (Email: Zidong.Wang@brunel.ac.uk).

Zhongyi Zhao is with the School of Mathematics, Southeast University, Nanjing 210096, China. (Email: zhaozy_sdust@163.com).

Hongli Dong is with the State Key Laboratory of Continental Shale Oil, Northeast Petroleum University, Daqing 163318, China; is also with the Artificial Intelligence Energy Research Institute, Northeast Petroleum University, Daqing 163318, China; and is also with the Heilongjiang Provincial Key Laboratory of Networking and Intelligent Control, Northeast Petroleum University, Daqing 163318, China. (Email: shiningdhl@vip.126.com).

often result in suboptimal bandwidth utilization and substantial quantization errors, particularly in scenarios characterized by pronounced signal dynamics. To overcome these limitations, dynamic quantization schemes have been developed, featuring adaptive threshold adjustment mechanisms that respond to real-time signal variations through intelligent scaling variables. This adaptive capability has attracted considerable research attention, with numerous studies demonstrating the superior performance of dynamic quantization in various control and estimation applications [23], [33], [34], [36], [37]. Notably, despite these demonstrated advantages, the integration of dynamic quantization techniques with state estimation algorithms for PDN applications remains largely unexplored in the existing literature, presenting both a research gap and opportunity for innovation.

The growing network openness in power systems has substantially increased cybersecurity vulnerabilities [9], [30], [31], [36], [40], [41], [44]. A notable case is the cyber-attacks on the Ukrainian power grid, which compromised system stability and resulted in significant economic damage [18], [24], [32]. Among prevalent cyber threats, denial-of-service (DoS) attacks and false data injection (FDI) attacks represent particularly critical challenges. DoS attacks are distinguished by their operational simplicity and high disruption potential, whereas FDI attacks are notable for their stealth characteristics. Existing research has developed various detection approaches to counter these threats [20], [22], [26]. Nevertheless, current methods typically depend on predetermined detection thresholds and demonstrate limited effectiveness against diverse attack variants. An alternative approach focuses on developing resilience filtering techniques to maintain estimation accuracy under attack conditions [8], [11], [15]. It is noteworthy that modern power systems face the compound threat of both DoS and FDI attacks, which cooperatively degrade system performance [19], [21]. To the best of our knowledge, existing research predominantly focuses on these attack modes in isolation, leaving a critical gap in understanding their combined effects.

Based on the preceding analysis, existing research has not adequately addressed PDN state estimation problems in the presence of DoS attacks, FDI attacks, and quantization effects. To address these challenges, this study proposes a dynamic quantization scheme and a novel recursive UKF algorithm specifically designed for PDNs that simultaneously accounts for quantization errors and hybrid cyber-attacks. This research confronts two fundamental challenges: 1) how to mathematically characterize the combined effect of dynamic quantization and hybrid attacks? and 2) how to design robust filtering algorithms capable of recursive implementation under these complex practical constraints? The principal contributions of this work are threefold:

1) A novel dynamic quantization scheme is proposed for digitizing power signals. Distinguished from conventional static uniform quantizers, this approach adapts to dynamic measurement variations by introducing time-varying scaling parameters, effectively eliminating potential saturation and deadband phenomena while minimizing quantization errors and maximizing bandwidth efficiency in data transmission.
2) A comprehensive state-space model for PDNs is established. This model explicitly incorporates nonlinear measurements, dynamic quantization effects, and the statistical coupling of hybrid cyber-attacks, providing a generalized framework for robust state estimation under complex scenarios.
3) A computationally efficient recursive UKF algorithm with real-time processing capability is developed. Its theoretical innovation lies in rigorously deriving a minimized upper bound for the estimation error covariance that comprehensively accounts for quantization, attacks, and measurement nonlinearity. Furthermore, it ensures estimation accuracy under complex dynamic conditions without requiring explicit detection.

The remainder of this paper is organized as follows. Section II establishes a comprehensive state-space model for PDNs that systematically incorporates dynamic quantization effects and hybrid cyber-attack scenarios, while outlining the primary research objectives. Section III presents the theoretical contributions, with particular focus on the development and analysis of a novel recursive UKF algorithm. Section IV provides extensive simulation studies that validate the efficacy of the proposed methodology, demonstrating its superior performance in terms of estimation accuracy and attack resilience across various operational scenarios. Finally, Section V concludes the paper by summarizing the key findings.

Notations: The symbol $\mathbb{R}^n$ denotes the n-dimensional Euclidean space, and $\mathbb{R}^{n\times m}$ represents the set of all real-valued matrices of dimension $n \times m$. The notation $\|*\|$ stands for the Euclidean norm of a vector or a matrix. The floor function $\lfloor x \rfloor$ indicates the largest integer not exceeding x. The symbol I corresponds to the identity matrix of appropriate dimensions. A block-diagonal matrix is expressed as $\mathrm{diag}\{*\}$. The Hadamard product is denoted by $\circ$, defined such that $[\mathscr{C}\circ\mathscr{D}]_{ij} = \mathscr{C}_i \cdot \mathscr{C}_j$ for matrices $\mathscr{C}$ and $\mathscr{D}$. For a square matrix M, M^T and M^{-1} refer to its transpose and inverse, respectively. Additionally, $M^{(\imath,\jmath)}$ signifies the $(\imath,\jmath)$-th element of the matrix M.

II. Problem Formulation and Preliminaries

A. State Space Model

This paper assumes that the power distribution system operates in a quasi-stable state condition. The selected state variables comprise the voltage magnitude $U_{i,k}$ and phase angle $\theta_{i,k}$ at each bus i ($i \in \{1, 2, \cdots, n\}$). Accordingly, the state vector $x_k \in \mathbb{R}^{2n}$ at time instant k is defined as follows:

$$x_k \triangleq \begin{bmatrix} U_{1,k} & U_{2,k} & \cdots & U_{n,k} & \theta_{1,k} & \theta_{2,k} & \cdots & \theta_{n,k} \end{bmatrix}^T.$$

The discrete-time model of the system is formulated as

$$x_k = A_{k-1}x_{k-1} + u_{k-1} + w_{k-1} \tag{1}$$

where the matrix A_{k-1} characterizes the transition rates between states, while the vector u_{k-1} captures the trend behavior of the state trajectory. These terms are derived via Holt's two-parameter exponential smoothing method. The process w_{k-1} represents a Gaussian white noise sequence with zero mean and covariance matrix $\mathcal{Q}_{k-1}$.

This article has been accepted for publication in a future issue of this journal, but has not been fully edited. Content may change prior to final publication.
Citation information: DOI: 10.1109/JIOT.2025.3610070, IEEE Internet of Things Journal

The deployment of high-precision phasor measurement units (PMUs) has significantly enhanced the measurement accuracy in modern power systems. However, the widespread adoption of PMUs in PDNs remains constrained by the considerable installation costs and the inherent topological complexity. To overcome these limitations while maintaining full network observability, this study adopts a hybrid measurement architecture that combines conventional distribution remote terminal units (DRTUs) with strategically deployed PMUs at critical buses. The measurement models for these two types of devices are formulated as follows:

1) For the ℓ-th PMU ($\ell \in \{1, 2, \cdots, m_p\}$) installed at bus ℓ, the measurement output $y_{p,\ell,k}$ is defined as $y_{p,\ell,k} \triangleq \begin{bmatrix} U_{\ell,k} & \theta_{\ell,k} \end{bmatrix}^T$. The ideal PMU measurement vector $y_{p,k} \in \mathbb{R}^{2m_p}$ is expressed as

$$y_{p,k} \triangleq \begin{bmatrix} y_{p,1,k}^T & y_{p,2,k}^T & \cdots & y_{p,m_p,k}^T \end{bmatrix}^T.$$

2) For the l-th DRTU ($l \in \{1, 2, \cdots, m_d\}$) installed at bus l, the measurement output $y_{d,l,k}$ is defined as

$$y_{d,l,k} \triangleq \begin{bmatrix} U_{l,k} & P_{l,k} & Q_{l,k} & P_{l\bar{l},k} & Q_{l\bar{l},k} \end{bmatrix}^T$$

where $P_{l,k}$ and $Q_{l,k}$ denote the active and reactive power injection measurements at bus l, while $P_{l\bar{l},k}$ and $Q_{l\bar{l},k}$ represent the active and reactive power flow measurements on the branch connecting buses l and $\bar{l}$. The physical relationships between these measurements and the system states are described by the following power flow equations:

$$P_{l\bar{l},k} = U_{l,k}^2 g_{l\bar{l}} - U_{l,k}U_{\bar{l},k}(g_{l\bar{l}} \cos\theta_{l\bar{l},k} + b_{l\bar{l}} \sin\theta_{l\bar{l},k}), \quad (2)$$

$$Q_{l\bar{l},k} = U_{l,k}U_{\bar{l},k}(b_{l\bar{l}} \cos\theta_{l\bar{l},k} - g_{l\bar{l}} \sin\theta_{l\bar{l},k}) - U_{l,k}^2 b_{l\bar{l}}, \quad (3)$$

$$P_{l,k} = \sum_{\bar{l}\in\mathcal{N}_l} P_{l\bar{l},k}, \quad Q_{l,k} = \sum_{\bar{l}\in\mathcal{N}_l} Q_{l\bar{l},k} \quad (4)$$

where $g_{l\bar{l}}$ and $b_{l\bar{l}}$ the series conductance and susceptance of the branch connecting buses l and $\bar{l}$; $\theta_{l\bar{l},k} \triangleq \theta_{l,k} - \theta_{\bar{l},k}$ indicates the phase angle difference between buses l and $\bar{l}$; and $\mathcal{N}_l$ denotes the set of buses adjacent to bus l (i.e., the neighborhood of bus l).

The ideal DRTU measurement vector $y_{d,k} \in \mathbb{R}^{5m_d}$ is expressed as

$$y_{d,k} \triangleq \begin{bmatrix} y_{d,1,k}^T & y_{d,2,k}^T & \cdots & y_{d,m_d,k}^T \end{bmatrix}^T.$$

By integrating measurements from both PMUs and DRTUs, the overall measurement vector $y_k \in \mathbb{R}^m$ ($m \triangleq 2m_p + 5m_d$) is formulated as $y_k \triangleq \begin{bmatrix} y_{p,k}^T & y_{d,k}^T \end{bmatrix}^T$. Taking into account measurement noises, the nonlinear measurement model is compactly represented as follows:

$$y_k = \mathrm{g}(x_k) + v_k \quad (5)$$

where $\mathrm{g}(\cdot) : \mathbb{R}^{2n} \to \mathbb{R}^m$ is the nonlinear measurement function determined by voltage magnitude $U_{\ell,k}$, phase angle $\theta_{\ell,k}$, and power flow and injection measurements governed by (2)-(4). v_k represents the Gaussian white noise with zero mean and covariance $\mathcal{R}_k$.

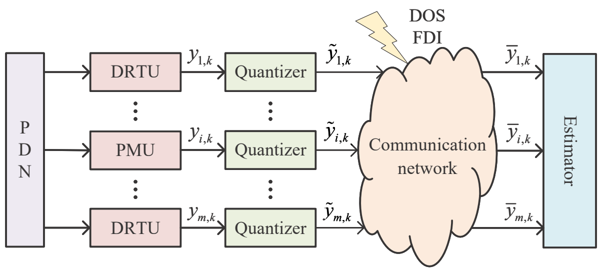

Fig. 1: The transmission of power signals with dynamic quantization schemes under hybrid cyber-attacks.

B. Dynamic Quantification Scheme

In modern digital communication systems for PDNs, quantization is a fundamental signal processing operation that transforms continuous analog measurements into discrete digital representations. This conversion enables robust data transmission from distributed measurement devices to centralized processing units, as illustrated in Fig. 1.

Consider a static uniform quantization scheme, where $y_{i,k} \in \mathbb{R}^{m_i}$ denotes the raw measurement vector from the i-th sensor ($i \in \{1, 2, \cdots, s\}$) at time instant k, and $\tilde{y}_{i,k}$ represents the corresponding quantized output. The quantization process is characterized by two key parameters: quantization ranges M_i and quantization errors Δ_i. Under normal operation (non-saturation regime), the quantization error $\varepsilon_{i,k} \triangleq \tilde{y}_{i,k} - y_{i,k}$ satisfies the boundedness condition $\|\varepsilon_{i,k}\| \leq \Delta_i$.

In practical engineering applications, the determination of appropriate quantization ranges M_i presents significant challenges, thereby limiting the effectiveness of conventional static quantizers. To address this limitation, this paper introduces an adaptive dynamic quantization scheme that automatically adjusts its quantization parameters based on real-time signal characteristics. The mathematical formulation of this dynamic quantizer is given as follows [34]:

$$\tilde{y}_{i,k} = \mu_{i,k} \left\lfloor \frac{y_{i,k}}{\mu_{i,k}} + \Delta_i \right\rfloor \quad (6)$$

where $\mu_{i,k}$ is the time-varying zoom parameter defined as $\mu_{i,k} \triangleq \frac{\vartheta\|y_{i,k}\|}{M_i}$ with $\vartheta > 1$. Under non-saturation conditions, the dynamic quantizer satisfies $\|\tilde{y}_{i,k} - y_{i,k}\| \leq \mu_{i,k}\Delta_i$.

Remark 1: Static uniform quantization, despite widely respected for implementation simplicity, suffers from inherent limitations in handling signals with significant amplitude variations. Specifically, high-amplitude signals frequently induce quantizer saturation, resulting in substantial distortion and potential information loss. Conversely, low-amplitude signals may fall within the deadband region, compromising the system sensitivity to crucial signal variations. In comparison, dynamic quantization schemes demonstrate superior performance by adaptively modify quantization parameters in real-time based on the observed signal characteristics [34], [42]. This adaptive mechanism enables effective handling of diverse signal amplitudes while mitigating saturation and deadband phenomena. As a result, dynamic quantization significantly enhances the precision and reliability of analog-to-digital conversion processes, making it particularly advantageous in complex power distribution systems.

C. Hybrid Attacks

The increasing openness of modern communication networks has heightened vulnerability of quantized signals to cyber-attacks. Practical incidents, such as the Ukraine power grid attack [32], confirms that adversaries are increasingly employing hybrid attack strategies (DoS and FDI) to maximize disruption. Following the established methodology [2], [21], we model the occurrence of these attacks via Bernoulli-distributed random variables $\lambda_{i,k}$ and $\tau_{i,k}$, achieving a balance between theoretical tractability and practical applicability. Although real attack patterns may exceed the scope of this model, its mathematical tractability provides the essential foundation for rigorous analysis. The probability distributions of these random variables are defined as follows:

$$\begin{aligned} &\Pr\{\lambda_{i,k}=1\}=\bar{\lambda}_i, \quad \Pr\{\lambda_{i,k}=0\}=1-\bar{\lambda}_i, \\ &\Pr\{\tau_{i,k}=1\}=\bar{\tau}_i, \quad \Pr\{\tau_{i,k}=0\}=1-\bar{\tau}_i \end{aligned}$$

where $\bar{\lambda}_i \in [0,1]$ and $\bar{\tau}_i \in [0,1]$ represent the probabilities of DoS and FDI attacks on the i-th channel, respectively.

To mitigate the detrimental effects of DoS attacks on measurement data integrity, this paper introduces a pseudo-measurement compensation mechanism that utilizes measurement prediction to reconstruct lost or corrupted data packets. Within this framework, the measurement $\bar{y}_k$ received by the remote filter is formulated as follows:

$$\bar{y}_k = \Lambda_k(\tilde{y}_k + (I-\mathcal{T}_k)\rho_k) + (I-\Lambda_k)\mathrm{g}(\hat{x}_{k|k-1}) \tag{7}$$

where

$$\begin{aligned} \bar{y}_k &\triangleq \begin{bmatrix} \bar{y}_{1,k}^T & \bar{y}_{2,k}^T & \cdots & \bar{y}_{s,k}^T \end{bmatrix}^T, \\ \tilde{y}_k &\triangleq \begin{bmatrix} \tilde{y}_{1,k}^T & \tilde{y}_{2,k}^T & \cdots & \tilde{y}_{s,k}^T \end{bmatrix}^T, \\ \Lambda_k &\triangleq \mathrm{diag}\{\lambda_{1,k}I, \lambda_{2,k}I, \cdots, \lambda_{s,k}I\}, \\ \mathcal{T}_k &\triangleq \mathrm{diag}\{\tau_{1,k}I, \tau_{2,k}I, \cdots, \tau_{s,k}I\}. \end{aligned}$$

Here, $\bar{y}_{i,k}$ denotes the measurement received by the remote estimator from the i-th sensor. The vector ρ_k represents the malicious injection signal introduced by potential FDI attacks, constrained by $\rho_k^T\rho_k \le \bar{\rho}$ with $\bar{\rho}$ being a predefined positive scalar that quantifies the maximum admissible attack magnitude. The term $\mathrm{g}(\hat{x}_{k|k-1})$ corresponds to the measurement prediction derived from the one-step state prediction $\hat{x}_{k|k-1}$.

Remark 2: The dynamic quantization process introduces errors ε_k into the quantization measurement $\tilde{y}_k$. During transmission, these signals are further compromised by hybrid cyber-attacks, including DoS attacks that randomly disrupt communication channels and FDI attacks that inject bounded malicious signals ρ_k. As a result, a statistical coupling arises in the measurement model, where quantization errors ε_k and the FDI attack signals are modulated by the DoS indicator Λ_k. This interdependence is mathematically captured by cross-terms such as $\mathbb{E}\{\Lambda_k\varepsilon_k\rho_k^T(I-\mathcal{T}_k)^T\}$ in (13), which explicitly quantifies the correlation between quantization inaccuracies and FDI attacks. Consequently, dynamic quantization and hybrid cyber-attacks jointly degrade estimation performance.

III. Design of Recursive UKF Algorithm

This section aims to develop a resilient filtering algorithm for PDNs subject to dynamic quantization effects and hybrid cyber-attacks. The designed filter is required to possess the following two key properties: 1) the filtering algorithm possess a recursive formulation to facilitate efficient online state estimation within PDNs; 2) despite the presence of nonlinear measurements and quantization effects, the state estimates achieve guaranteed precision characterized by a bounded estimation error covariance

Before presenting the main results, several foundational lemmas are introduced to support the subsequent discussions.

Lemma 1: [28] For any real matrices $\mathcal{X}$ and $\mathcal{Y}$ and an arbitrary positive scalar σ, the following matrix inequality holds:

$$\mathcal{X}\mathcal{Y}^T + \mathcal{Y}\mathcal{X}^T \le \sigma\mathcal{X}\mathcal{X}^T + \sigma^{-1}\mathcal{Y}\mathcal{Y}^T$$

Lemma 2: [10] Let $C = \mathrm{diag}\{c_1, c_2, \cdots, c_q\}$ be a random diagonal matrix with $\{c_i\}_{i=1}^q$ as its diagonal elements, and A be a real-valued matrix, the following equality holds:

$$\mathrm{E}\{CAC^T\} = \begin{bmatrix} \mathrm{E}\{c_1^2\} & \mathrm{E}\{c_1c_2\} & \cdots & \mathrm{E}\{c_1c_q\} \\ \mathrm{E}\{c_2c_1\} & \mathrm{E}\{c_2^2\} & \cdots & \mathrm{E}\{c_2c_q\} \\ \vdots & \vdots & \ddots & \vdots \\ \mathrm{E}\{c_qc_1\} & \mathrm{E}\{c_qc_2\} & \cdots & \mathrm{E}\{c_q^2\} \end{bmatrix} \circ A$$

Lemma 3: [43] Consider two positive definite symmetric matrices X, Y, and a function $\mathcal{H}_k(\cdot)$ satisfying $\mathcal{H}_k(\cdot) = \mathcal{H}_k^T(\cdot) \in \mathbb{R}^{n\times n}$. If $\mathcal{H}_k(X) \le \mathcal{H}_k(Y)$ holds for all $X \le Y$, then the solutions M_k and N_k to the following difference equations

$$M_{k+1} \le \mathcal{H}_k(M_k), \quad N_{k+1} = \mathcal{H}_k(N_k),$$

with initial condition $M_0 = N_0 > 0$, satisfy $M_k \le N_k$ for all $k \ge 0$.

Following the established prediction-correction framework [4], [7], [46], we construct a recursive filter. The prediction step utilizes the system dynamics model (1) to generate a prior state estimate. The update step then corrects this estimate using the actual received measurement $\bar{y}_k$ in (7) (which is quantized and potentially compromised by cyber-attacks) and the predicted measurement $\mathrm{g}(\hat{x}_{k|k-1})$ derived from measurement equations (bus voltage, branch current, branch power).

$$\hat{x}_{k|k-1} = A_{k-1}\hat{x}_{k-1} + u_{k-1}, \tag{8}$$

$$\hat{x}_k = \hat{x}_{k|k-1} + K_k(\bar{y}_k - \mathrm{g}(\hat{x}_{k|k-1})) \tag{9}$$

where $\hat{x}_k$ denotes the state estimate and K_k represents the filter gain matrix to be designed.

Define the prediction error $e_{k|k-1} \triangleq x_k - \hat{x}_{k|k-1}$ and the filtering error $e_k \triangleq x_k - \hat{x}_k$. The prediction errors stems from the propagation of prior estimation errors and process noise (accounting for uncertainties in generation forecasts and system dynamics). The estimation error combines the effects of prediction error and measurement residuals. According to the system model (1), the measurement (7), and the filter (8)-(9), the prediction error $e_{k|k-1}$ and the filtering error e_k at time instant k are derived as follows:

$$e_{k|k-1} = A_{k-1}e_{k-1} + w_{k-1}, \tag{10}$$

This article has been accepted for publication in a future issue of this journal, but has not been fully edited. Content may change prior to final publication.
Citation information: DOI: 10.1109/JIOT.2025.3610070, IEEE Internet of Things Journal

$$e_k = e_{k|k-1} - K_k\Lambda_k(\Gamma_k + \varepsilon_k + (I-\mathcal{T}_k)\rho_k + v_k) \tag{11}$$

where

$$\Gamma_k \triangleq \mathrm{g}(x_k) - \mathrm{g}(\hat{x}_{k|k-1}),$$
$$\varepsilon_k \triangleq \begin{bmatrix}\varepsilon_{1,k}^T & \varepsilon_{2,k}^T & \cdots & \varepsilon_{s,k}^T\end{bmatrix}^T.$$

Define the prediction error covariance and filtering error covariance as $P_{k|k-1} \triangleq \mathrm{E}\{e_{k|k-1}e_{k|k-1}^T\}$ and $P_k \triangleq \mathrm{E}\{e_k e_k^T\}$, respectively. The prediction error covariance is driven by the system dynamics uncertainty and process noise. The filtering error covariance is significantly more complex due to the hybrid attacks and quantization, which quantifies the expected squared estimation error for the bus voltages and angles. Based on the error system (10)-(11), we arrive at

$$P_{k|k-1} = A_{k-1}P_{k-1}A_{k-1}^T + \mathcal{Q}_{k-1}, \tag{12}$$

$$\begin{aligned} P_k = {} & P_{k|k-1} + K_k(\mathrm{E}\{\Lambda_k\Gamma_k\Gamma_k^T\Lambda_k^T\} \\ & + \mathrm{E}\{\Lambda_k(I-\mathcal{T}_k)\rho_k\rho_k^T(I-\mathcal{T}_k)^T\Lambda_k^T\} \\ & + \mathrm{E}\{\Lambda_k\varepsilon_k\varepsilon_k^T\Lambda_k^T\} + \mathrm{E}\{\Lambda_k v_k v_k^T\Lambda_k^T\})K_k^T \\ & - \mathrm{E}\{e_{k|k-1}\Gamma_k^T\Lambda_k^T\}K_k^T - K_k\mathrm{E}\{\Lambda_k\Gamma_k e_{k|k-1}^T\} \\ & - \Theta_{1,k} - \Theta_{1,k}^T - \Theta_{2,k} - \Theta_{2,k}^T \\ & + \Theta_{3,k} + \Theta_{3,k}^T + \Theta_{4,k} + \Theta_{4,k}^T \end{aligned} \tag{13}$$

where

$$\begin{aligned} \Theta_{1,k} &\triangleq \mathrm{E}\{e_{k|k-1}\varepsilon_k^T\Lambda_k^T\}K_k^T, \\ \Theta_{2,k} &\triangleq \mathrm{E}\{e_{k|k-1}\rho_k^T(I-\mathcal{T}_k)^T\Lambda_k^T\}K_k^T, \\ \Theta_{3,k} &\triangleq K_k\mathrm{E}\{\Lambda_k\varepsilon_k\rho_k^T(I-\mathcal{T}_k)^T\Lambda_k^T\}K_k^T, \\ \Theta_{4,k} &\triangleq K_k\mathrm{E}\{\Lambda_k\varepsilon_k v_k^T\Lambda_k^T\}K_k^T. \end{aligned}$$

Remark 3: Due to the coupling of multiple factors, including quantization errors, attack signals, measurement noise, and measurement nonlinearity, through stochastic attack indicators, cross-terms inevitably arise in the filtering error covariance, which complicate the accurate determination of P_k. Consequently, deriving a guaranteed upper bound $\bar{P}_k$ becomes a practical alternative for ensuring the stability and robustness in PDN state estimation. Although this bound may be conservative, it rigorously ensures that the estimation error variance remains bounded by $\bar{P}_k$ in the mean-square sense. This provides a quantifiable safety assurance for grid operations that rely on accurate state estimates for monitoring and control.

Theorem 1: Considering the system model (1), the measurement (7), and the filter (8)-(9), there exist positive constants σ_ι ($\iota \in \{1,2,3,4\}$) such that, under initial condition $P_0 = \bar{P}_0 > 0$, the following recursive relations admit positive definite solutions:

$$\bar{P}_{k|k-1} = A_{k-1}\bar{P}_{k-1}A_{k-1}^T + \mathcal{Q}_{k-1}, \tag{14}$$

$$\begin{aligned} \bar{P}_k = {} & \delta_1\bar{P}_{k|k-1} + K_k\Xi_k K_k^T - \mathrm{E}\{e_{k|k-1}\Gamma_k^T\} \\ & \times \bar{\Lambda}_k K_k^T - K_k\bar{\Lambda}_k\mathrm{E}\{\Gamma_k e_{k|k-1}^T\} \end{aligned} \tag{15}$$

where

$$\begin{aligned} \Xi_k \triangleq {} & \hat{\Lambda}_k \circ \mathrm{E}\{\Gamma_k\Gamma_k^T\} + \delta_2\hat{\Lambda}_k \circ \left(\sum_{i=1}^{s}(\mu_{i,k}\Delta_i)^2 I\right) \\ & + \delta_3\tilde{\Lambda}_k \circ (\bar{\rho}I) + \delta_4\hat{\Lambda}_k \circ \mathcal{R}_k, \\ \hat{\Lambda}_k^{(\imath,\jmath)} \triangleq {} & \mathrm{E}\{\Lambda_k^{(\imath,\imath)}\Lambda_k^{(\jmath,\jmath)}\}, \\ \tilde{\Lambda}_k^{(\imath,\jmath)} \triangleq {} & \mathrm{E}\{\Lambda_k^{(\imath,\imath)}(\mathrm{I}-\mathcal{T}_k^{(\imath,\imath)})\Lambda_k^{(\jmath,\jmath)}(\mathrm{I}-\mathcal{T}_k^{(\jmath,\jmath)})\}, \\ \bar{\Lambda}_k \triangleq {} & \mathrm{diag}\{\bar{\lambda}_1 I, \bar{\lambda}_2 I, \cdots, \bar{\lambda}_s I\}, \\ \delta_1 \triangleq {} & 1 + \sigma_1 + \sigma_2, \quad \delta_2 \triangleq 1 + \sigma_1^{-1} + \sigma_3 + \sigma_4, \\ \delta_3 \triangleq {} & 1 + \sigma_2^{-1} + \sigma_3^{-1}, \quad \delta_4 \triangleq 1 + \sigma_4^{-1}. \end{aligned}$$

Under the given conditions, $\bar{P}_k$ is an upper bound for the filtering error covariance P_k, satisfying the matrix inequality $P_k \le \bar{P}_k$. The upper $\bar{P}_k$ is then minimized through the appropriate design of the filter gain matrix K_k:

$$K_k = \mathrm{E}\{e_{k|k-1}\Gamma_k^T\}\bar{\Lambda}_k\Xi_k^{-1}. \tag{16}$$

Proof: By using Lemma 1 and Lemma 2, the following inequality relationships are established:

$$-\Theta_{1,k} - \Theta_{1,k}^T \le \sigma_1 P_{k|k-1} + \sigma_1^{-1}K_k \times \hat{\Lambda}_k \circ \mathrm{E}\{\varepsilon_k\varepsilon_k^T\}K_k^T, \tag{17}$$

$$-\Theta_{2,k} - \Theta_{2,k}^T \le \sigma_2 P_{k|k-1} + \sigma_2^{-1}K_k \times \tilde{\Lambda}_k \circ \mathrm{E}\{\rho_k\rho_k^T\}K_k^T, \tag{18}$$

$$\Theta_{3,k} + \Theta_{3,k}^T \le \sigma_3 K_k\hat{\Lambda}_k \circ \mathrm{E}\{\varepsilon_k\varepsilon_k^T\}K_k^T + \sigma_3^{-1}K_k\tilde{\Lambda}_k \circ \mathrm{E}\{\rho_k\rho_k^T\}K_k^T, \tag{19}$$

$$\Theta_{4,k} + \Theta_{4,k}^T \le \sigma_4 K_k\hat{\Lambda}_k \circ \mathrm{E}\{\varepsilon_k\varepsilon_k^T\}K_k^T + \sigma_4^{-1}K_k\hat{\Lambda}_k \circ \mathcal{R}_k K_k^T. \tag{20}$$

Furthermore, the quantization error ε_k and the attack signal ρ_k satisfy the following inequalities:

$$\mathrm{E}\{\varepsilon_k\varepsilon_k^T\} \le \mathrm{E}\{\varepsilon_k^T\varepsilon_k I\} \le \sum_{i=1}^{s}(\mu_{i,k}\Delta_i)^2 I, \tag{21}$$

$$\mathrm{E}\{\rho_k\rho_k^T\} \le \mathrm{E}\{\rho_k^T\rho_k I\} \le \bar{\rho}I. \tag{22}$$

Substituting equations (17)-(22) into (13) yields

$$\begin{aligned} P_k \le {} & \delta_1 P_{k|k-1} + K_k\Xi_k K_k^T - \mathrm{E}\{e_{k|k-1}\Gamma_k^T\} \\ & \times \bar{\Lambda}_k^T K_k^T - K_k\bar{\Lambda}_k\mathrm{E}\{\Gamma_k e_{k|k-1}^T\}. \end{aligned} \tag{23}$$

This indicates that the filtering error covariance P_k is bounded above by $\bar{P}_k$, satisfying the conditions of Lemma 3. Consequently, it can be concluded that $P_k \le \bar{P}_k$.

By applying the completing-the-square technique, the upper bound matrix $\bar{P}_k$ can be reformulated as

$$\begin{aligned} \bar{P}_k = {} & (K_k - \mathrm{E}\{e_{k|k-1}\Gamma_k^T\}\bar{\Lambda}_k\Xi_k^{-1})\Xi_k(K_{k+1} \\ & - \mathrm{E}\{e_{k|k-1}\Gamma_k^T\}\bar{\Lambda}_k\Xi_k^{-1})^T - \mathrm{E}\{e_{k|k-1}\Gamma_k^T\}\bar{\Lambda}_k \\ & \times \Xi_k^{-1}\bar{\Lambda}_k\mathrm{E}\{\Gamma_k e_{k|k-1}^T\} + \delta_1\bar{P}_{k|k-1}. \end{aligned} \tag{24}$$

The formula (24) reveals that the matrix $\bar{P}_k$ attains its minimum value when the filter gain is designed according to (16), thus completing the proof. ■

As established in Theorem 1, we have derived the upper bound for the filtering error covariance P_k and the filter gain K_k. Nevertheless, the explicit expressions for the expectations $\mathrm{E}\{\Gamma_k\Gamma_k^T\}$ and $\mathrm{E}\{e_{k|k-1}\Gamma_k^T\}$ remain to be determined. To address this challenge, we employ the unscented transformation technique to approximate the probability densities of the

This article has been accepted for publication in a future issue of this journal, but has not been fully edited. Content may change prior to final publication.
Citation information: DOI: 10.1109/JIOT.2025.3610070, IEEE Internet of Things Journal

nonlinear function $\mathrm{g}(x_k)$, thereby enabling the derivation of these critical expectation terms. The detailed derivation and implementation procedures are presented as follows.

At time instant $k-1$, the filtering error covariance P_{k-1} is substituted with its upper bound matrix $\bar{P}_{k-1}$. Subsequently, a set of $2n+1$ sigma points are generated using the symmetric proportionality-corrected sampling method, defined as follows:

$$\mathcal{X}_{\varsigma,k-1} = \begin{cases} \hat{x}_{k-1}, \varsigma = 0, \\ \hat{x}_{k-1} + \sqrt{(n+\lambda)\bar{P}_{k-1}}, \\ \quad \varsigma = 1, 2, \cdots, n, \\ \hat{x}_{k-1} - \sqrt{(n+\lambda)\bar{P}_{k-1}}, \\ \quad \varsigma = n+1, n+2, \cdots, 2n \end{cases} \tag{25}$$

where $\lambda \triangleq \alpha^2(n+\kappa) - n$ with $\alpha \in [0,1]$ and $\kappa \geq 0$.

The mean weight ω_ς and the covariance weight φ_ς for the sigma points are calculated by the following equations:

$$\begin{cases} \omega_\varsigma = \dfrac{\lambda}{n+\lambda}, & \varsigma = 0, \\ \varphi_\varsigma = \dfrac{\lambda}{n+\lambda} + (1-\alpha^2+\beta), & \varsigma = 0, \\ \omega_\varsigma = \varphi_\varsigma = \dfrac{1}{2(n+\lambda)}, & \varsigma = 1, 2, \cdots, 2n \end{cases} \tag{26}$$

where β is a positive scalar.

These sigma points $\chi_{\varsigma,k|k-1}$ are propagated through the state-transition function, as described by equation (1), to obtain the transformed sigma points $\mathcal{X}_{\varsigma,k|k-1}$:

$$\mathcal{X}_{\varsigma,k|k-1} = A_{k-1}\mathcal{X}_{\varsigma,k-1} + u_{k-1}. \tag{27}$$

Next, these sigma points are passed through the measurement function $\mathrm{g}(\cdot)$ to derive the measurement prediction sigma points $\mathcal{Y}_{\varsigma,k|k-1}$:

$$\mathcal{Y}_{\varsigma,k|k-1} = \mathrm{g}(\mathcal{X}_{\varsigma,k|k-1}), \quad \varsigma = 0, 1, \cdots, 2n. \tag{28}$$

By using the weighted average method, the measurement prediction $\hat{z}_{k|k-1}$ and the terms $\mathrm{E}\{\Gamma_k\Gamma_k^T\}$ and $\mathrm{E}\{e_{k|k-1}\Gamma_k^T\}$are derived by the following formulas:

$$\hat{z}_{k|k-1} = \sum_{\varsigma=0}^{2n} \omega_\varsigma \mathcal{Y}_{\varsigma,k|k-1}, \tag{29}$$

$$\begin{aligned} \mathrm{E}\{\Gamma_k\Gamma_k^T\} = &\sum_{\varsigma=0}^{2n} \varphi_\varsigma (\mathcal{Y}_{\varsigma,k|k-1} - \hat{z}_{k|k-1}) \\ &\times (\mathcal{Y}_{\varsigma,k|k-1} - \hat{z}_{k|k-1})^T, \end{aligned} \tag{30}$$

$$\begin{aligned} \mathrm{E}\{e_{k|k-1}\Gamma_k^T\} = &\sum_{\varsigma=0}^{2n} \varphi_\varsigma (\mathcal{X}_{\varsigma,k|k-1} - \hat{x}_{k|k-1}) \\ &\times (\mathcal{Y}_{\varsigma,k|k-1} - \hat{z}_{k|k-1})^T. \end{aligned} \tag{31}$$

It is noteworthy that the relation $\mathrm{E}\{\Gamma_k e_{k|k-1}^T\} = \mathrm{E}\{(e_{k|k-1}\Gamma_k^T)^T\}$ holds, which allows for the straightforward derivation of the term $\mathrm{E}\{\Gamma_k e_{k|k-1}^T\}$. By substituting equations (30)-(31) into (15) and (16), the upper bound matrix $\bar{P}_k$ and the filter gain matrix K_k can be derived.

Remark 4: This study develops a resilient filtering framework for PDNs subject to dynamic quantization effects and hybrid cyber-attacks through four key technical approaches. First, a dynamic quantization mechanism employing time-varying scaling factors is introduced to mitigate saturation and deadband phenomena. Second, hybrid cyber-attacks and inherent quantization errors modeled through a unified measurement framework governed by Bernoulli-distributed random sequences. Third, the matrix inequality in Lemma 1 is applied to handle uncertain cross-terms, and the unscented transformation is utilized to approximate expectation terms $\mathrm{E}\{\Gamma_k\Gamma_k^T\}$ and $\mathrm{E}\{e_{k|k-1}\Gamma_k^T\}$ without relying on linearization approximations. Finally, an upper bound for the filtering error covariance is derived by solving Riccati-like difference equations, and a filter gain is designed based on the minimum variance criterion.

Remark 5: Unlike detection-based methodologies that rely on explicit attack identification, our approach adopts a detection-free resilience strategy based on unified uncertainty modeling. Specifically, the proposed filtering algorithm introduces three key advancements: 1) hybrid attacks and quantization errors are jointly modeled as compound uncertainties in the measurement model; 2) an upper bound on the filtering error covariance is derived through elegant treatment of uncertain cross-terms; and 3) a recursive UKF framework tailored for PDNs ensures real-time processing capability. This approach eliminates explicit detection modules, thereby reducing computational overhead and avoiding detection delays. By emphasizing robust estimation rather than attack detection, the strategy maintains real-time performance without sacrificing resilience.

In what follows, the developed recursive UKF algorithm under dynamic quantization effects and hybrid attacks is summarized in Algorithm 1.

Algorithm 1 Recursive UKF Algorithm Under Dynamic Quantization Effects and Hybrid Attacks

1: Set the initial state vector $\hat{x}_0$ and the covariance matrix P_0.
2: Calculate the state prediction $\hat{x}_{k|k-1}$ and the associated covariance matrix $\bar{P}_{k|k-1}$ using (8) and (14), respectively.
3: Generate $2n+1$ sigma points from (25) by replacing P_{k-1} with $\bar{P}_{k-1}$, and determine the mean weights ω_ς and the covariance weight φ_ς according to (26).
4: Propagate the sigma points through the state-transition function (27) to obtain transformed samples, and compute the measurement prediction sigma points $\mathcal{Y}_{\varsigma,k|k-1}$ using (28).
5: Obtain the measurement prediction $\hat{z}_{k|k-1}$ from (29), and calculate the expectation terms $\mathrm{E}\{\Gamma_k\Gamma_k^T\}$ and $\mathrm{E}\{e_{k|k-1}\Gamma_k^T\}$ via (30) and (31), respectively.
6: Determine the filter gain matrix K_k by (16).
7: Update the state estimate $\hat{x}_k$ and the covariance matrix $\bar{P}_k$ according to (9) and (15), respectively.
8: Set $k = k+1$. If $k > k_{\max}$, end; Otherwise go to step 2.

IV. Simulation Results and Analysis

To validate the effectiveness of the proposed methodology, simulations are conducted on a three-phase balance system

This article has been accepted for publication in a future issue of this journal, but has not been fully edited. Content may change prior to final publication.
Citation information: DOI: 10.1109/JIOT.2025.3610070, IEEE Internet of Things Journal

(IEEE 69 distribution test system) and a three-phase unbalance system (IEEE 34 distribution test system), where topological configurations are illustrated in Fig. 2 and [14]. All simulations are conducted on a PC with an Intel Core i5-1155G7 processor (2.50 GHz) and 16GB RAM using MATLAB R2018b. The experimental framework employs a daily load curve with one-minute interval to emulate realistic operational conditions in urban PDNs. System states are generated through detailed power flow calculations, with additive Gaussian noise to represent measurement uncertainties inherent in practical scenarios.

To comprehensively evaluate the robustness of the proposed filtering algorithm, we conduct systematic simulations under multiple operational scenarios, which consider various noise conditions, attack probabilities, and quantization parameters. The system are configured as follows: the initial error covariance $P_0 = 10^{-6} I_n$ and the process noise covariance $Q_k = 10^{-6} I_n$. The algorithm parameters are set as $\sigma_1 = 0.1$, $\sigma_2 = 0.5$, $\sigma_3 = 0.05$, $\sigma_4 = 3.5$, $\alpha = 0.01$, $\beta = 2$, $\kappa = 0$, and $\vartheta = 1.05$. The quantization and attack parameters are set as $\bar{\rho} = 0.45$, $M = 100$, $\bar{\lambda}_i = 0.95$, and $\bar{\tau}_i = 0.7$.

The filtering accuracy is evaluated using root mean square error (RMSE) and mean square error (MSE) metrics, defined as $\mathrm{MSE}_k \triangleq \frac{1}{2n} \sum_{i=1}^{2n} (x_{i,k} - \hat{x}_{i,k})^2$ and $\mathrm{RMSE}_k \triangleq \sqrt{\mathrm{MSE}_k}$, where $x_{i,k}$ and $\hat{x}_{i,k}$ denote the i-th element of the state vector x_k and its estimate and n indicates the total number of buses in the system.

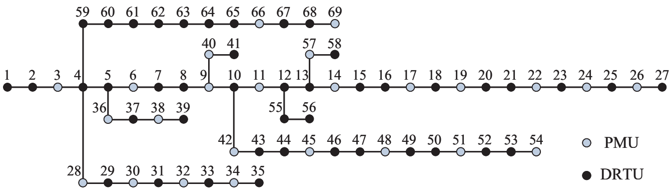

Fig. 2: The topological structure of the IEEE 69 distribution test system.

A. Algorithm Verification Using IEEE 69 Balance System

The effectiveness of the proposed algorithm is evaluated through comparative simulations against Cauchy kernel-based maximum correntropy filtering (MCF), UKF, and cubature Kalman filtering (CKF). Under Gaussian noise conditions ($R_k = \mathrm{diag}10^{-4} I_{2m_p}, 10^{-6} I_{5m_d}$), Fig. 3 compares the estimation performance of voltage magnitude and phase angle at bus 17, and Fig. 4 presents the corresponding RMSE values. The results demonstrate the superior estimation accuracy of the proposed algorithm over the other methods. This improvement is attributed to the explicit incorporation of quantization effects and hybrid cyber-attacks into the filter design. As shown in Fig. 5, the Log(RMSE) of the proposed algorithm consistently remains below its theoretically derived upper bound. This behavior, achieved through effective handling of uncertainty terms, confirms the robustness and reliability of the proposed approach.

Consider a non-Gaussian measurement noise scenario modeled by the following mixture distribution:

$$v_k \sim 0.4\mathcal{N}\{0, \mathrm{diag}\{10^{-4} I_{2m_p}, 10^{-6} I_{5m_d}\}\}$$
$$+ 0.6\mathcal{N}\{0, \mathrm{diag}\{10^{-2} I_{2m_p}, 10^{-4} I_{5m_d}\}\}.$$

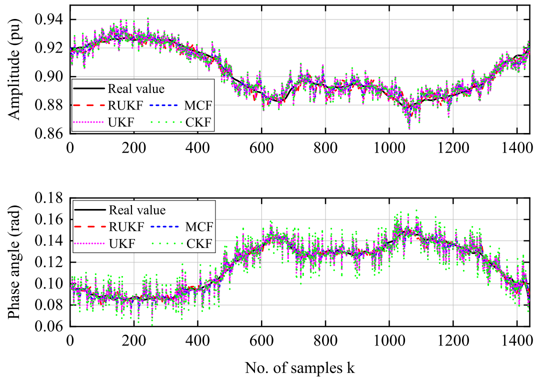

Fig. 3: Estimated voltage amplitudes and phase angles at bus 17 under Gaussian noise conditions.

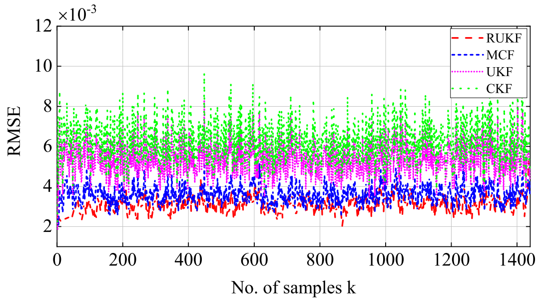

Fig. 4: RMSE values of different filtering algorithm under Gaussian noise conditions.

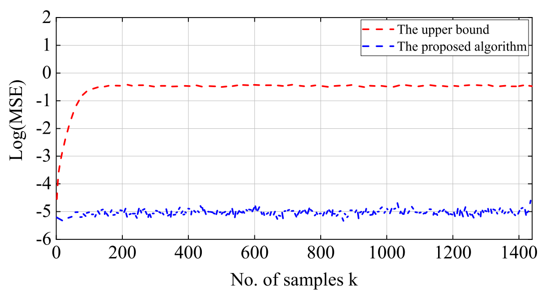

Fig. 5: Log(MSE) and its upper bound.

Fig. 6 shows the estimated voltage magnitude and phase angle at bus 9, and Fig. 7 presents the corresponding RMSE values. The results indicate that the proposed method and MCF achieve similar estimation accuracy, and both outperform UKF and CKF. This further demonstrates the effectiveness of the proposed method under non-Gaussian noise conditions.

B. Algorithm Verification Using IEEE 34 Unbalance System

To demonstrate the effectiveness of the proposed method, the IEEE 34 three-phase unbalanced distribution system is employed, with five photovoltaic power generation units integrated into the system. Similar to subsection IV-A, simulations are conducted under both Gaussian and non-Gaussian noise conditions. Under Gaussian noise, Fig. 8 presents the estimated voltage amplitude and phase angle for phase C at bus 850, while Fig. 9 shows the corresponding RMSE values. For the

This article has been accepted for publication in a future issue of this journal, but has not been fully edited. Content may change prior to final publication.
Citation information: DOI: 10.1109/JIOT.2025.3610070, IEEE Internet of Things Journal

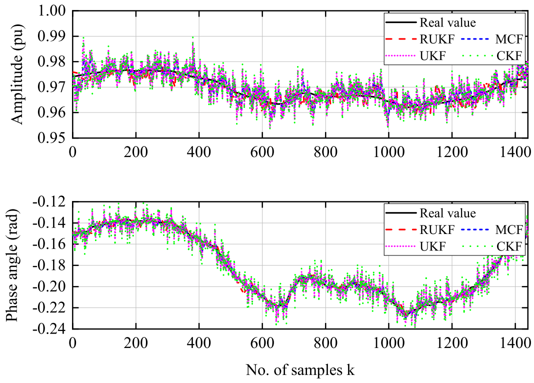

Fig. 6: Estimated voltage amplitudes and phase angles at bus 9 under non-Gaussian noise conditions.

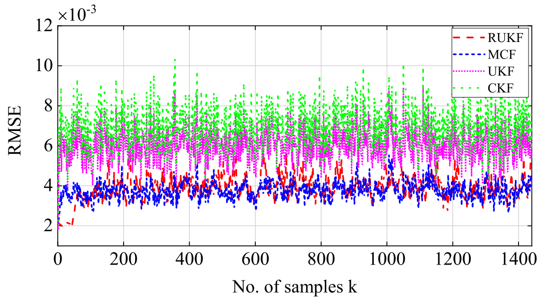

Fig. 7: RMSE values of different filtering algorithm under non-Gaussian noise conditions.

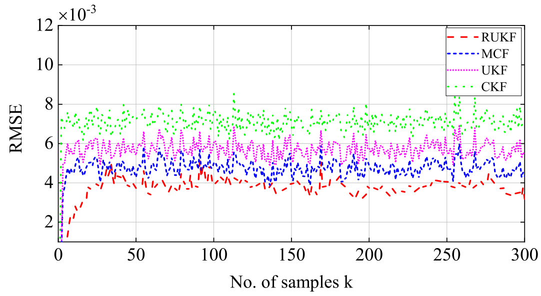

Fig. 9: RMSE values under Gaussian noise conditions.

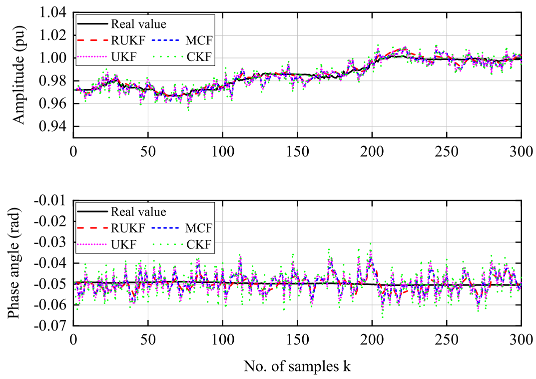

Fig. 10: Estimated voltage amplitudes and phase angles of A-phase at bus 48 under non-Gaussian noise conditions.

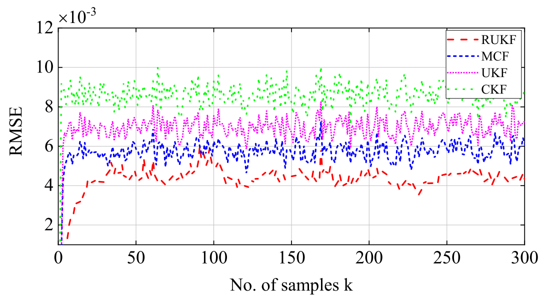

Fig. 11: RMSE values under non-Gaussian noise conditions.

non-Gaussian case, using the noise distribution defined in subsection IV-A, Fig. 10 displays the voltage magnitude and phase angle estimates for phase A at bus 834, and Fig. 11 provides the associated RMSE results. As shown in Figs. 8-11, the proposed method achieves higher estimation accuracy compared with other algorithms under both noise conditions. Notably, the estimation error of the proposed method does not increase significantly even under intensified noise, confirming its robustness in complex noise environments.

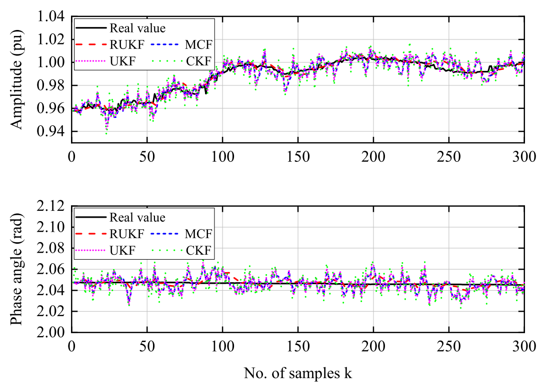

Fig. 8: Estimated voltage amplitudes and phase angles of C-phase at bus 22 under Gaussian noise conditions.

C. Estimation Performance Under Different Attack Scenarios

In order to evaluate the resilience of the proposed method under adversarial conditions, we specifically design three attack scenarios with different intensity levels while maintaining fixed quantization parameters. Fig. 12 demonstrates the reliable estimation performance by showing RMSE values of the proposed method across all attack scenarios. The experimental results clearly reveal the superior estimation accuracy of the proposed algorithm despite the presence of adversarial interference, showcasing its strong resilience against hybrid attacks. This robustness highlights the method's capability to ensure operational stability in challenging environments, making it particularly suitable for practical applications.

D. Estimation Performance With Different Quantizers

A comprehensive performance comparison between dynamic and static uniform quantization schemes validates the advantages of the proposed method. The experimental evaluation considers two distinct configurations: 1) both schemes operating at identical quantization levels ($L_i = 500$ with $L_i \triangleq \frac{M_i}{\Delta_i}$), and 2) dynamic quantization with $L_i = 500$ versus static quantization with $L_i = 1000$. Fig. 13 illustrates

Citation information: DOI: 10.1109/JIOT.2025.3610070, IEEE Internet of Things Journal

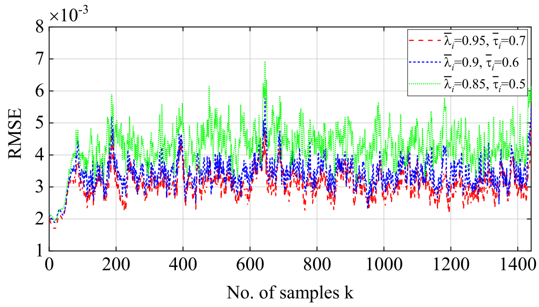

Fig. 12: RMSE values under different attack rates.

the comparative RMSE values under equal quantization levels, while Fig. 14 presents the results for the case where the static quantizer operates at twice the quantization level.

The experimental results in Figs. 13-14 demonstrate that the proposed dynamic quantization scheme achieves comparable estimation accuracy to conventional static quantization while requiring only half the quantization levels. Specifically, the dynamic approach maintains equivalent estimation performance with a 50% reduction in quantization requirements, thereby significantly conserving communication bandwidth without compromising measurement accuracy. These findings clearly indicate that the dynamic quantization strategy strike a trade-off between communication resource utilization and estimation performance.

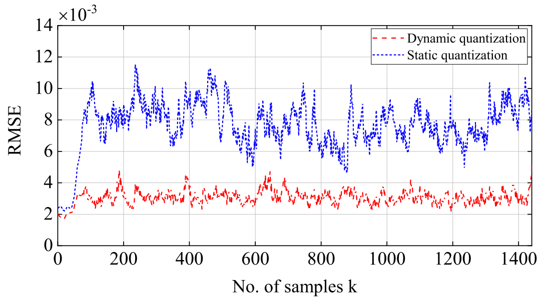

Fig. 13: RMSE values under the same quantization level.

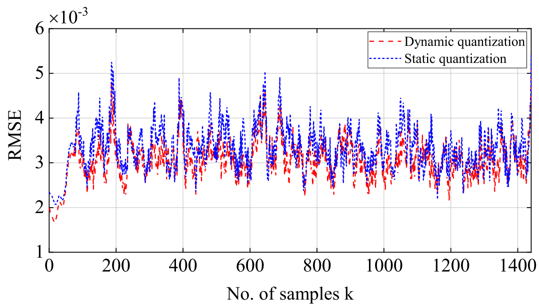

Fig. 14: RMSE values under different quantization levels.

V. Conclusion

This paper has addressed the state estimation challenge for PDNs under simultaneous quantization effects and hybrid cyber-attacks. To optimize signal digitization, a novel dynamic quantization scheme has been adopted to adaptively adjusts the quantization range and quantization errors through innovative deflation variables. The hybrid attack scenarios, comprising DoS and FDI attacks, have been characterized using Bernoulli distributed random variables. By leveraging the unscented transformation technique, we have derive a theoretically guaranteed upper bound for the filtering error covariance, which forms the foundation for our proposed recursive UKF algorithm. The effectiveness of the proposed filtering algorithm has been validated through extensive simulations conducted on the IEEE 69 distribution test system, with comparative results demonstrating significant improvements in estimation accuracy and attack resilience compared with conventional approaches. Future research topics include 1) investigating state estimation and control problems under non-Gaussian noise conditions [29], [35], [39], [45]; and 2) extending the main results to multi-area PDNs under communication constraints [3], [13], [25]; and 3) exploring cubature Kalman fusion filtering problem under amplify-and-forward relays [16].

References

[1] S. Azuma and T. Sugie, Synthesis of optimal dynamic quantizers for discrete-valued input control, *IEEE Transactions on Automatic Control*, vol. 53, no. 9, pp. 2064–2075, Oct. 2008.

[2] R. Caballero-Águila, M. P. Frías-Bustamante and A. Oya-Lechuga, Least-squares linear estimation for multirate uncertain systems subject to DoS attacks, *International Journal of Network Dynamics and Intelligence*, vol. 4, no. 2, art. no. 100014, Jun. 2025.

[3] W. Chen, J. Hu, Z. Wu and S. Ma, A survey on fault detection for networked systems under communication constraints, *Systems Science & Control Engineering*, vol. 13, no. 1, art. no. 2460434, 2025.

[4] D. Dai, J. Li, Y. Song and F. Yang, Event-based recursive filtering for nonlinear bias-corrupted systems with amplify-and-forward relays, *Systems Science & Control Engineering*, vol. 12, no. 1, art. no. 2332419, 2024.

[5] H. Fang, M. A. Haile and Y. Wang, Robust extended Kalman filtering for systems with measurement outliers, *IEEE Transactions on Control Systems Technology*, vol. 30, no. 2, pp. 795–802, Mar. 2022.

[6] S. Feng, X. Li, S. Zhang, Z. Jian, H. Duan and Z. Wang, A review: State estimation based on hybrid models of Kalman filter and neural network, *Systems Science & Control Engineering*, vol. 11, no. 1, art. no. 217368, Dec. 2023.

[7] P. Gao, C. Jia and A. Zhou, Encryption-decryption-based state estimation for nonlinear complex networks subject to coupled perturbation, *Systems Science & Control Engineering*, vol. 12, no. 1, art. no. 2357796, 2024.

[8] X. Gao, F. Deng, W. Shang, X. Zhao and S. Li, Attack-resilient asynchronous state estimation of interval type-2 fuzzy systems under stochastic protocol, *International Journal of Systems Science*, vol. 55, pp. 2688–2700, Oct. 2024.

[9] A. Hasan, I. Kuncara, A. Widyotriatmo, O. Osen and R. T. Bye, Secure state estimation and control for autonomous ships under cyberattacks, *Systems Science & Control Engineering*, vol. 13, no. 1, art. no. 2518964, 2025.

[10] R. A. Horn and C. R. Johnson, Topic in Matrix Analysis. New York, NY, USA: Cambridge Univ. Press, 1991.

[11] F. Jin, L. Ma, C. Zhao and Q. Liu, A quantization-coding scheme with variable data rates for cyber-physical systems under DoS attacks, *Systems Science & Control Engineering*, vol. 12, no. 1, art. no. 2348690, May 2024.

[12] M. A. Khan and B. Hayes, Smart meter based two-layer distribution system state estimation in unbalanced MV/LV networks, *IEEE Transactions on Industrial Informatics*, vol. 18, no. 1, pp. 688–697, Jan. 2022.

[13] C. Li, Y. Liu, M. Gao and L. Sheng, Fault-tolerant formation consensus control for time-varying multi-agent systems with stochastic communication protocol, *International Journal of Network Dynamics and Intelligence*, vol. 3, no. 1, art. no. 100004, Mar. 2024.

[14] G. Li, Z. Wang, X. Bai, Z. Zhao and H. Dong, Event-triggered set-membership filtering for active power distribution systems under fading channels: A zonotope-based approach, *IEEE Transactions on Automation Science and Engineering*, vol. 22, pp. 1139–1151, 2025.

This article has been accepted for publication in a future issue of this journal, but has not been fully edited. Content may change prior to final publication.
Citation information: DOI: 10.1109/JIOT.2025.3610070, IEEE Internet of Things Journal

[15] J. Li, Y. Suo, S. Chai, Y. Xu and Y. Xia, Resilient and event-triggered control of singular Markov jump systems against cyber attacks, *International Journal of Systems Science*, vol. 55, no. 2, pp. 222–236, 2024.
[16] J. Li, Z. Wang, J. Hu, H. Dong and H. Liu, Cubature Kalman fusion filtering under amplify-and-forward relays with randomly varying channel parameters, *IEEE/CAA Journal of Automatica Sinica*, vol. 12, no. 2, pp. 356–368, Feb. 2025.
[17] S. Li, Y. He, H. Wu and M. Ding, Dynamic state estimation for distribution networks based on adaptive set membership filter under unknown but bounded noise environments, *IEEE Sensors Journal*, vol. 24, no. 8, pp. 12654–12666, Apr. 2024.
[18] G. Liang, S. R. Weller, J. Zhao, F. Luo and Z. Dong, The 2015 ukraine blackout: Implications for false data injection attacks, *IEEE Transactions on Power Systems*, vol. 32, no. 4, pp. 3317–3318, Jul. 2017.
[19] J. Liu, Y. Gu, L. Zha, Y. Liu and J. Cao, Event-triggered H_∞ load frequency control for multiarea power systems under hybrid cyber attacks, *IEEE Transactions on Intelligent Transportation Systems*, vol. 49, no. 8, pp. 1665–1678, Aug. 2019.
[20] X. Liu and Z. Li, False data attacks against AC state estimation with incomplete network information, *IEEE Transactions on Smart Grid*, vol. 8, no. 5, pp. 2239–2248, Sept. 2017.
[21] L. Ma, H. Zhang, G. Wang, C. Yang and L. Zhou, Security coordination control for the belt conveyor systems with false data injection attacks, *International Journal of Network Dynamics and Intelligence*, vol. 4, no. 1, art. no. 100001, Mar. 2025.
[22] A. Mohammadi and K. N. Plataniotis, Noncircular attacks on phasor measurement units for state estimation in smart grid, *IEEE Journal of Selected Topics in Signal Processing*, vol. 12, no. 4, pp. 777–789, Aug. 2018.
[23] L. Montestruque and P. Antsaklis, Static and dynamic quantization in model-based networked control systems, *ISA Transactions*, vol. 80, no. 1, pp. 87–101, Jan. 2007.
[24] W. Qian, D. Lu, S. M. Guo and Y. J. Zhao, Distributed state estimation for mixed delays system over sensor networks with multichannel random attacks and markov switching topology, *IEEE Transactions on Neural Networks and Learning Systems*, vol. 35, no. 6, pp. 8623–8637, 2024.
[25] W. Qian, Y. M. Wu and J. Q. Yang, Event-driven reduced-order fault detection filter design for nonlinear systems with complex communication channel, *IEEE Transactions on Fuzzy Systems*, vol. 32, no. 1, pp. 281–293, 2024.
[26] Z. Qu, J. Yang, Y. Lang, Y. Wang, X. Han and X. Guo, Earth-mover-distance-based detection of false data injection attacks in smart grids, *Energies*, vol. 15, no. 5, Feb. 2022, art. no. 1773.
[27] F. Shabani, M. Seyedyazdi, M. Vaziri, M. Zarghami and S. Vadhva, State estimation of a distribution system using WLS and EKF techniques, *Proceedings of the IEEE International Conference on Information Reuse and Integration*, San Francisco, 2015, pp. 609–613.
[28] Y. Shen and S. Sun, Distributed recursive filtering for multi-rate uniform sampling systems with packet losses in sensor networks, *International Journal of Systems Science*, vol. 54, no. 8, pp. 1729–1745, Jun. 2023.
[29] Z. Sun and C. Han, Linear state estimation for multi-rate NCSs with multi-channel observation delays and unknown Markov packet losses, *International Journal of Network Dynamics and Intelligence*, vol. 4, no. 1, art. no. 100005, Mar. 2025.
[30] E. Tian, H. Chen, C. Wang and L. Wang, Security-ensured state of charge estimation of lithium-ion batteries subject to malicious attacks, *IEEE Transactions on Smart Grid*, vol. 14, no. 3, pp. 2250–2261, May 2023.
[31] E. Tian, M. Fan, L. Ma and D. Yue, Stochastic important-data-based attack power allocation against remote state estimation in sensor networks, *IEEE Transactions on Automatic Control*, vol. 70, no. 3, pp. 2012–2019, Mar. 2025.
[32] C. Vellaithurai, A. Srivastava, S. Zonouz and R. Berthier, CPIndex: Cyber-physical vulnerability assessment for power-grid infrastructures, *IEEE Transactions on Smart Grid*, vol. 6, no. 2, pp. 566–575, Mar. 2015.
[33] F. Wang, Z. Wang, J. Liang and C. Silvestre, Recursive locally minimum-variance filtering for two-dimensional systems: when dynamic quantization effect meets random sensor failure, *Automatica*, vol. 148, art. no. 110762, Feb. 2023.
[34] S. Wang, Z. Wang, H. Dong and Y. Chen, Distributed state estimation under random parameters and dynamic quantizations over sensor networks: A dynamic event-based approach, *IEEE Transactions on Signal and Information Processing over Networks*, vol. 6, pp. 732–743, 2020.
[35] Y. Wang, Z. Wang, L. Zou, Q. Ge and H. Dong, Asynchronous PID control for T-S fuzzy systems over Gilbert-Elliott channels utilizing detected channel modes, *IEEE Transactions on Fuzzy Systems*, vol. 33, no. 5 pp. 1555–1567, May 2025.
[36] Y. Wang and S. Yu, An improved dynamic quantization scheme for uncertain linear networked control systems, *Automatica*, vol. 92, pp. 244–248, Jun. 2018.
[37] Y.-A. Wang, Z. Wang, L. Zou, B. Shen and H. Dong, Detection of perfect stealthy attacks on cyber-physical systems subject to measurement quantizations: a watermark-based strategy, *IEEE/CAA Journal of Automatica Sinica*, vol. 12, no. 1, pp. 114–125, Jan. 2025.
[38] S. Wei, J. Xu, Z. Wu, Q. Hu and X. Yu, A false data injection attack detection strategy for unbalanced distribution networks state estimation, *IEEE Transactions on Smart Grid*, vol. 14, no. 5, pp. 3992–4006, Sept. 2023.
[39] C. Xian, Y. Zhao, Z.-G. Wu, G. Wen and J.-A. Pan, Event-triggered distributed average tracking control for lipschitz-type nonlinear multiagent systems, *IEEE Transactions on Cybernetics*, vol. 53, no. 2, pp. 779–792, Feb. 2023.
[40] J. Yang, W. A. Zhang and F. Guo, Adaptive distributed Kalman-like filter for power system with cyber attacks, *Automatica*, vol. 137, Mar. 2022, art. no. 110091.
[41] L. Yu, Z. Wang, Y. Liu and C. Xue, Sampled-data nonfragile bipartite tracking consensus for nonlinear multiagent systems: dealing with denial-of-service attacks, *IEEE Transactions on Systems, Man, and Cybernetics: Systems*, vol. 55, no. 2, pp. 1202–1214, Feb. 2025.
[42] Y. Hu, C. Zhang and S. Liu, Privacy-preserving distributed recursive filtering for state-saturated systems with quantization effects, *International Journal of Network Dynamics and Intelligence*, vol. 4, no. 2, art. no. 100012, Jun. 2025.
[43] Y. Theodor and U. Shaked, Robust discrete-time minimum-variance filtering, *IEEE Transactions on Signal Processing*, vol. 44, no. 2, pp. 181–189, 1996.
[44] H. Yu, Z. Wang, L. Zou and Y. Wang, A survey on security control and estimation for cyber-physical systems under cyber-attacks: Advances, challenges and future directions, *Artificial Intelligence Science and Engineering*, vol. 1, no. 1, pp.1-16, 2025.
[45] M. Yuan and W. Qian, Adaptive output feedback tracking control for nonlinear systems with unknown growth rate, *International Journal of Network Dynamics and Intelligence*, vol. 3, no. 1, art. no. 100002, Mar. 2024.
[46] R. Zhang, H. Liu, Y. Liu and H. Tan, Dynamic event-triggered state estimation for discrete-time delayed switched neural networks with constrained bit rate, *Systems Science & Control Engineering*, vol. 12, no. 1, art. no. 2334304, 2024.
[47] J. Zhao and L. Mili, Robust unscented Kalman filter for power system dynamic state estimation with unknown noise statistics, *IEEE Transactions on Smart Grid*, vol. 10, no. 2, pp. 1215–1224, Mar. 2019.
[48] Z. Zhao, Z. Wang and L. Zou, Sequential fusion estimation for multirate complex networks with uniform quantization: A zonotopic set-membership approach, *IEEE Transactions on Neural Networks and Learning System*, vol. 35, no. 4, pp. 5764–5777, Apr. 2024.

Xingzhen Bai was born in Shandong, China, in 1977. He received the B.Sc. degree in electrical technology and the M.Sc. degree in power electronics and power drives from the Shandong University of Science and Technology, Qingdao, China, in 2000 and 2006, respectively, and the Ph.D. degree in computer software and theory from Tongji University, Shanghai, China, in 2010. He is currently a Professor with the College of Electrical Engineering and Automation, Shandong University of Science and Technology. His current research interests include distributed estimation and control, wireless sensor networks, and smart grids.

This article has been accepted for publication in a future issue of this journal, but has not been fully edited. Content may change prior to final publication.
Citation information: DOI: 10.1109/JIOT.2025.3610070, IEEE Internet of Things Journal

Guhui Li received the B.Sc. degree in electrical engineering and automation from the College of Electrical Engineering and Automation, Qilu University of Technology, Jinan, China, in 2020, and the M.Sc. degree in electrical engineering and automation from the Shandong University of Science and Technology, Qingdao, China, in 2023, where he is currently pursuing the Ph.D. degree in control science and engineering. From February 2025 to August 2025, he was a Research Assistant with the Department of Electrical Engineering, City University of Hong Kong, Hong Kong, China. His current research interests include distributed estimation and control and its application in power distribution networks.

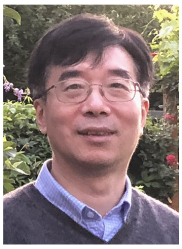

Zidong Wang (Fellow, IEEE) received the B.Sc. degree in mathematics from Suzhou University, Suzhou, China, in 1986, and the M.Sc. degree in applied mathematics and the Ph.D. degree in electrical engineering from the Nanjing University of Science and Technology, Nanjing, China, in 1990 and 1994, respectively.

He is currently a Professor in dynamical systems and computing with the Department of Computer Science, Brunel University London, Uxbridge, U.K. From 1990 to 2002, he held teaching and research appointments in universities in China, Germany, and the U.K. He has published a number of articles in international journals. His research interests include dynamical systems, signal processing, bioinformatics, control theory and applications.

Prof. Wang is a Holder of the Alexander von Humboldt Research Fellowship of Germany, the JSPS Research Fellowship of Japan, and William Mong Visiting Research Fellowship of Hong Kong. He serves (or has served) as the Editor-in-Chief for *International Journal of Systems Science*, *Neurocomputing*, and *Systems Science & Control Engineering*; and an Associate Editor for 12 international journals, including IEEE Transactions on Automatic Control, IEEE Transactions on Control Systems Technology, IEEE Transactions on Neural Networks, IEEE Transactions on Signal Processing, and IEEE Transactions on Systems, Man, and Cybernetics-Part C. He is a member of the Academia Europaea and European Academy of Sciences and Arts, an Academician of the International Academy for Systems and Cybernetic Sciences, a fellow of the Royal Statistical Society, and a member of program committee for many international conferences.

Zhongyi Zhao (Member, IEEE) received the B.Eng. degree in electrical engineering and automation in 2016 and the Ph.D. degree in control theory and control engineering in 2023, both from the Shandong University of Science and Technology, Qingdao, China. He is currently a Postdoctoral Research Fellow with the School of Mathematics, Southeast University, Nanjing, China. From November 2021 to October 2022, he was a visiting Ph.D. student with the Department of Computer Science, Brunel University London, Uxbridge, U.K. His current research interests include networked systems, multi-sensor information fusion, and set-membership estimation.

Hongli Dong (Senior Member, IEEE) received the Ph.D. degree in control science and engineering from the Harbin Institute of Technology, Harbin, China, in 2012.

From 2009 to 2010, she was a Research Assistant with the Department of Applied Mathematics, City University of Hong Kong, Hong Kong. From 2010 to 2011, she was a Research Assistant with the Department of Mechanical Engineering, The University of Hong Kong, Hong Kong. From 2011 to 2012, she was a Visiting Scholar with the Department of Information Systems and Computing, Brunel University London, Uxbridge, U.K. From 2012 to 2014, she was an Alexander von Humboldt Research Fellow with the University of Duisburg–Essen, Duisburg, Germany. She is currently a Professor with the Artificial Intelligence Energy Research Institute, Northeast Petroleum University, Daqing, China. She is also the Director of the Heilongjiang Provincial Key Laboratory of Networking and Intelligent Control, Daqing, China. Her current research interests include robust control and networked control systems.

Prof. Dong is a very active reviewer for many international journals.